AIAA AVIATION Forum
22-26 June 2015, Dallas, TX
21st AIAA/CEAS Aeroacoustics Conference

10.2514/6.2015-2541

Towards Cascade Trailing-Edge Noise Modeling Using a Mode-Matching Technique

Michel Roger*, Benjamin François†
École Centrale de Lyon
Laboratoire de Mécanique des Fluides et Acoustique, UMR CNRS 5509
36, avenue Guy de Collongue, 69143 Écully, France

Stéphane Moreau ‡
Département de Génie Mécanique, Université de Sherbrooke
Sherbrooke, QC, J1K2R1, Canada

An original analytical mode-matching technique is proposed to formulate the problem of the broadband trailing-edge noise produced by outlet guide vanes in an axial-flow fan architecture. The trailing-edge noise sources are not vane-to-vane correlated but their radiation is determined by a cascade effect that must be accounted for. This is achieved here in the frequency domain and in two dimensions for a preliminary assessment of the method. In a first step the trailing-edge noise sources of a single vane are shown to be equivalent to the onset of a so-called edge dipole, the direct field of which is expanded in a series of plane-wave modes. In a second step the diffraction of each mode is derived considering the cascade as an array of bifurcated waveguides and using a mode-matching technique. The cascade response is finally synthesized by summing the diffracted fields of all modes. The interest of the approach is that it can be extended to a three-dimensional annular configuration. As such it is a promising and versatile alternative to previously published methods.

Nomenclature

$\bar{a}_j$, a_j	pressure and potential coefficients for plane waves
A_m^j, B_s^j	transmitted and reflected mode amplitudes, single interface
c	chord length
c_0	sound speed
D_m^0, U_m^0	downstream and upstream mode amplitudes in the channels
E, F	Fresnel integral and related function
h	inter-vane channel height
$k = \omega/c_0$	acoustic wavenumber
$K = k/\beta$	scaled wavenumber
$K^{(j)}$	axial wavenumber in the channels
K_m	incident axial wavenumber
$\bar{K}_s^j$	effective axial wavenumbers of reflected/transmitted waves
M_0	axial Mach number
p, p_0	acoustic pressure
r_c	radius of the unwrapped cut of the stator
(r_0, θ_0), (r, θ)	source and observer cylindrical coordinates around an edge

*Professor, AIAA Member, michel.roger@ec-lyon.fr
†Postdoctoral research fellow, AIAA Member
‡Professor, AIAA Lifetime Member

$(\bar{r}_0, \bar{\theta}_0)$, $(\bar{r}, \bar{\theta})$	same coordinates corrected for convection
$\bar{R}$	corrected source-to-observer distance
R_s, T_s	reflected and transmitted mode amplitudes, double interface
V	vane number
v_x	acoustic axial velocity
$\mathbf{v}_K^h$	hydrodynamic velocity associated to the Kutta condition
(x, y)	axial and transverse Cartesian coordinates
$X = x/\beta$	scaled coordinate
α_s^j	scattered transverse wavenumbers of transmitted/reflected waves
$\beta = \sqrt{1 - M_0^2}$	compressibility parameter
$\mathbf{\Gamma}$	pressure and axial-velocity vector
ϕ	acoustic potential
ρ_0	fluid density
$\mathbf{\Omega_K}$, Ω_K, Ω_0	vorticity generated by the Kutta condition

Subscripts and superscripts

$(-)_0$	source-point coordinate
$(-)^0$	reference channel
$(-)_j$	incident wave index
$(-)_m$	channel mode index
$(-)_K$	Kutta-condition associated quantity
$(-)_s$	reflected or transmitted wave index
$(-)_{i,r,t,u,d}$	incident, reflected, transmitted, upstream and downstream potentials
$(-)^{\pm}$	for downstream/upstream wavenumbers
$\mathrm{e}^{-\mathrm{i}\,\omega\, t}$	time dependance of monochromatic waves

I. Introduction

The design of many axial-flow fans involves a rotor and a downstream row of stationary outlet guide vanes called stator. The aerodynamic noise of the rotor-stator system is caused by various aerodynamic interactions. According to the acoustic analogy and for subsonic Mach numbers, sound mainly originates from fluctuating lift forces on the blades and the vanes, all acting as equivalent dipoles. The lift fluctuations are induced by time variations of the velocity relative to the blades/vanes. The main declination of this mechanism is the wake-interaction noise produced as the wakes of the rotor blades impinge on the stator vanes. The mean velocity deficit and the turbulence in the wakes generate tonal noise and broadband noise, respectively, the sources of which are distributed on the vanes. Independently the turbulent boundary layers developing on the blades and the vanes are scattered as sound at the trailing edges, also contributing to the broadband noise. That trailing-edge noise is not blade-to-blade or vane-to-vane correlated, which means that the sound generation takes places in the same way as for an isolated airfoil. But the sound radiation away from the trailing-edge area is more or less dramatically restructured by multiple scattering on ajacent blades/vanes. This restructuration referred to as the cascade effect is the main motivation of the present work. The emphasis is on the trailing-edge noise of the stator, though the same approach could be transposed to a rotor.

In most architectures the outlet guide vanes are moderately cambered and staggered at leading edge, and nearly parallel to the axis at trailing edge. As a result they have a large overlap and can be viewed from downstream as an array of parallel and zero-stagger plates. When trying to reproduce aeroacoustic phenomena using analytical approaches, the cascade effect of the stator appears as a key feature to deal with. The cascade effect is not only involved in the sound generation process but also when the sound generated by the rotor blades is transmitted downstream in the exhaust duct, especially for stators with a large number of vanes and quite large hub-to-tip ratios. Many works contributed to the development of analytical or semi-analytical cascade response functions for sound generation or transmission in blade rows, amongst others the approach by Glegg[5] and Posson*et al*[14] selected here for the discussion. But only wake-interaction noise or turbulence-impingement noise is generally considered. The cascade effect on the trailing-edge noise mechanism is more difficult to formulate even though an attractive and elegant approach has been proposed by Glegg & Jochault.[6] The issue is that trailing-edge noise sources are localized and poorly correlated, which makes them difficult to describe in a cascade context. Though only outlet guide vanes are considered in the present work, the same would hold for the blades of a rotor except that most often the overlap is smaller, at least in the tip region of the blades, and that the number of blades is also smaller. Furthermore the stagger angle of the blades is quite large. The case of the stator is chosen here because the equivalent cascade will be assumed with zero stagger for simplicity. This simplification could be released in a future work.

The aforementioned approach by Glegg,[5] Glegg & Jochault[6] and Posson *et al*[14] relies on an extensive use of the Wiener-Hopf technique formulated in a Cartesian reference frame for a rectilinear cascade. This means that the investigated annular cascade must be split into a series of thin annuli that are unwrapped and treated separately. Arbitrary stagger angle, sweep and lean can be accounted for by changing the parameters in each strip. In contrast no simple equivalent in cylindrical coordinates is available and as a result adjacent blades or vanes are artificially considered as parallel plates. The present approach is proposed as an alternative. It is based on a mode-matching technique, considering a blade/vane row as a periodic array of bifurcated waveguides. It can be transposed easily in a three-dimensional context in cylindrical coordinates for the analysis of annular cascades. A previous, still incomplete attempt dealing with sound transmission at the inlet of a centrifugal compressor is described by Ingenito & Roger.[11] Another application to the outer part of the compressor and to the associated radial vaned diffuser has been considered by Roger *et al*[18] in polar coordinates, based on the use of spiral waves in a spiral base flow. This versatility is an attractive advantage since the splitting of a machine into strips is avoided, but it is balanced by the limitation that blade/vane twist or other design features cannot be simply considered. The two-dimensional extension to staggered vanes is straightforward as suggested by similar works in electromagnetic wave theory.[20] Finally the Wiener-Hopf technique and the mode-matching technique are mathematically equivalent when addressing rigid-plate cascade problems in two dimensions. One or the other is presumably better suited depending on the design features when three-dimensional blade/vane rows are modeled.

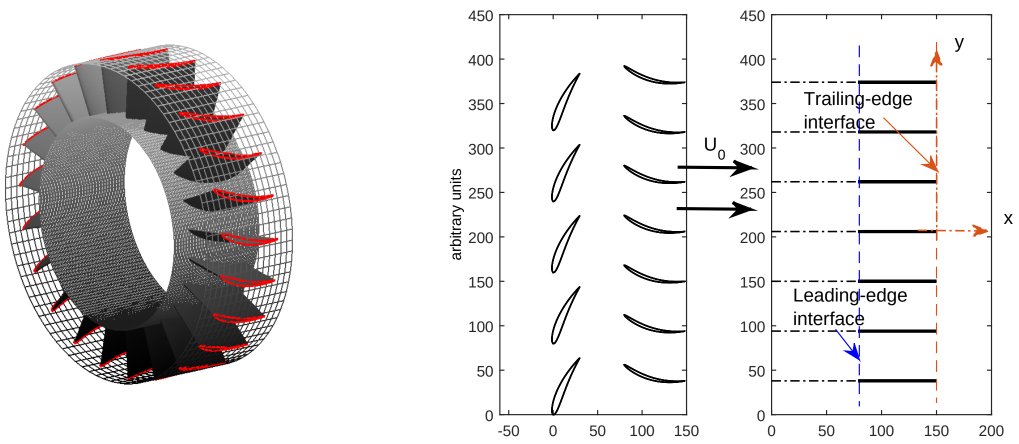

(a) (b)

Figure 1: (a): typical axial-flow stator architecture. (b): unwrapped representation showing the rotor blades (left) and the equivalent rectilinear cascade of plates mimicking the stator (right).

The present investigation remains two-dimensional but it must be understood as the first step of a methodology that will be progressively generalized and implemented in a unified three-dimensional model of axial-flow turbomachine. The stator vanes are assumed parallel, axially aligned and zero-stagger plates (Fig.1). They are equivalent to a periodic array of channels with rigid walls. As a principle, it is stated that the trailing-edge noise sources of an isolated vane can be reproduced by introducing an equivalent lift dipole approached very close to the trailing edge from downstream and diffracted by the edge. This intuition is a key step of the approach; its validity is confirmed in section A. It is guided by the fact that trailing-edge noise physics develops in the very vicinity of the trailing edge and radiates waves of opposite phases on both sides of the plate. The equivalent excitation of the trailing-edge interface of the stator in terms of acoustic plane-wave modes is next derived in section B. The response of the stator as a waveguide system is addressed for isolated incident modes and for the complete field of the trailing-edge dipole in section III, where fundamental scattering properties are discussed. Finally the application of the methodology to predict broadband trailing-edge noise is introduced in section IV.

II. Edge-Dipole Formulation

A. Tuning of the Equivalent Dipole

The mode-matching procedure is based on the idea that the trailing-edge noise sources of an isolated vane can be described with an equivalent point dipole approached at a very close distance to the edge from downstream. A key point of the model for future use is to determine the strength of this dipole. This is achieved by comparing the exact field the dipole would generate close to the edge of a rigid half-plane to Amiet's solution currently used to model trailing-edge noise of isolated thin airfoils. More precisely the comparison is made on the wall-pressure distribution that is the trace of the sound field, rather than on the sound field itself.

The field of the dipole in the presence of the half-plane is derived from the exact two-dimensional half-plane Green's function in the presence of flow, introduced by Jones[12] and re-addressed by Rienstra.[15] Only the transverse component of the first gradient of the Green's function with respect to source coordinates is needed because the dipole of interest is oriented normal to the flow direction. If no additional Kutta condition is imposed at the edge the Green's function reads, for a flow of Mach number M_0 in the positive x direction

$$G_M(x,y,k) \;=\; \frac{1}{\beta}\,\mathrm{e}^{-\mathrm{i}\,K\,M\,(X-X_0)}\,G^{(1/2)}(X,y,K)$$

with

$$G^{(1/2)}(X,y,K) \;=\; \int_{-\infty}^{s_1} \mathrm{e}^{\mathrm{i}\,K\,\bar r_1\,\sqrt{1+u^2}}\,\frac{\mathrm{d}u}{\sqrt{1+u^2}} \;+\; \int_{-\infty}^{s_2} \mathrm{e}^{\mathrm{i}\,K\,\bar r_2\,\sqrt{1+u^2}}\,\frac{\mathrm{d}u}{\sqrt{1+u^2}}\,. \tag{1}$$

In this expression $\bar r_{1,2}^2 \;=\; \bar r^2 + \bar r_0^2 - 2\,\bar r \bar r_0\,\cos(\bar\theta \mp \bar\theta_0)$, $\bar r = \sqrt{X^2+y^2}$ being the corrected observer distance to the edge involving the stretched coordinate $X = x/\beta$, with $\beta = \sqrt{1-M_0^2}$, and $K = k/\beta$. The angles $\bar\theta$ and $\bar\theta_0$ are defined as the corrected angles from the wake direction $x > 0$, and

$$s_1 \;=\; \frac{2\,\sqrt{\bar r_0\,\bar r}}{\bar r_1}\,\cos\frac{\bar\theta-\bar\theta_0}{2} \qquad\qquad s_2 \;=\; -\,\frac{2\,\sqrt{\bar r_0\,\bar r}}{\bar r_2}\,\cos\frac{\bar\theta+\bar\theta_0}{2}$$

Though it admits a simplified expression for a point source approaching the edge in such a way that $k\,\bar r_0$ takes arbitrary small values, the exact implementation has been used here. The field of the dipole is known to exhibit the typical cardioid pattern in this case, with phase opposition on both sides of the half-plane, zero sound in the wake and maximum sound upstream.[17] This feature is imposed by the asymptotics of the Green's function itself and would hold for various positions of the source, though the equivalent dipole is chosen here at zero θ_0 angle. Only the trace of the pressure field at the wall is needed in the present study. It is plotted as the thick red dashed line in Fig. 2. It is worth noting that Jones[12] and Rienstra[15] also consider an optional Kutta condition in the form of the additional term

$$G_K(x,y,k) \;=\; \frac{A_K}{2}\,\frac{\mathrm{e}^{\mathrm{i}\,\pi/4}}{\sqrt{\pi}}\,\mathrm{e}^{-\mathrm{i}\,K\,\bar r}\,\left[\mathrm{F}\left(\sqrt{2\,K\bar r}\,\sin\frac{\bar\theta-\bar\theta_1}{2}\right) + \mathrm{F}\left(\sqrt{2\,K\bar r}\,\sin\frac{\bar\theta+\bar\theta_1}{2}\right)\right]$$

$$-\,\frac{A_K}{2}\,2\,\mathrm{e}^{-\mathrm{i}\,K X/M_0}\,\cosh\left(\frac{\beta\,K}{M_0}\,y\right)\,\mathrm{H}(-y) \tag{2}$$

where the factor A_K is given by Jones as

$$\frac{A_K}{2} \;=\; \mathrm{sign}(y_0)\,\sqrt{\frac{2\,\pi}{K\,\bar r_0}}\,\sqrt{1-\frac{X_0}{\bar r_0}}\,\sqrt{\frac{M_0}{1+M_0}}\,\mathrm{e}^{-\mathrm{i}\,K\,\bar r_0\,-\mathrm{i}\,\pi/4}$$

and where $\bar{\theta}_1$ is an imaginary angle such that $\cos\bar{\theta}_1 = 1/M_0$. H is the Heaviside function and F is the complex function of complex argument defined by

$$\mathrm{F}(z) = \mathrm{e}^{\mathrm{i}\,z^2} \int_z^\infty \mathrm{e}^{-\mathrm{i}\,t^2}\,dt = \frac{\sqrt{\pi}}{2}\,\mathrm{e}^{-\mathrm{i}\,\pi/4}\,\mathrm{e}^{\mathrm{i}\,z^2}\,\mathrm{erfc}\left(\mathrm{e}^{\mathrm{i}\,\pi/4}\,z\right)$$

This term is known to cause amplification of the radiated field for small values of $k\,\bar{r}_0$ and significant values of the Mach number.[17] The complete result including it is plotted for completeness as the thin red dashed line in Fig. 2, where a phase shift is also noticed.

Amiet's formulation of trailing-edge noise in the frequency domain[2,16] provides directly an expression for the radiating wall-pressure produced by the primary scattering of boundary-layer vorticity into sound at the edge. This pressure field must be distinguished from the incident hydrodynamic pressure associated with the convected turbulence in the boundary layers. The latter is the origin of the former but does not enter the problem statement explicitly. Assuming an infinite chord, that pressure is distributed according to the expression

$$P_1(x) = A\,\mathrm{e}^{\mathrm{i}\,\alpha\,K_1 X}\,\left[(1-\mathrm{i})\,\mathrm{E}\left(-\left[\alpha\,K_1 + (1+M_0)\,\mu\right]\,X\right) - 1\right] \tag{3}$$

if the same convention $\mathrm{e}^{-\mathrm{i}\,\omega\,t}$ is chosen everywhere for monochromatic waves. Equation (3) refers to the two-dimensional response for a single gust or Fourier component of the incident hydrodynamic pressure, of amplitude A. α, estimated here around 1.25, is the flow-speed to convection-speed ratio, $K_1 = \omega/(\beta U_0)$ is the aerodynamic wavenumber and $\mu = K_1 M_0/\beta$. E is the Fresnel integral defined as

$$\mathrm{E}(\xi) = \int_0^\xi \frac{\mathrm{e}^{\mathrm{i}\,t}}{\sqrt{2\,\pi\,t}}\,\mathrm{d}t$$

A is used together with a phase-quadrature factor $\mathrm{e}^{\mathrm{i}\,\pi/4}$ as a tuning parameter to make the expression of Eq. (3) coincide at best with the field produced by Eq. (1) and the tuned Amiet's solution is plotted as the blue line in Fig. 2. It is found in a good agreement with the trace of the equivalent point dipole. In a statistical declination of Amiet's trailing-edge noise model the gust amplitude A would be related to the hydrodynamic wall-pressure spectrum taken closely upstream of the trailing-edge and to its spanwise correlation length.[16] Another tuning could produce a similar fit with the solution including the Kutta correction. The figure confirms that a point dipole can be used to describe the sources of trailing-edge noise with a reasonable accuracy.

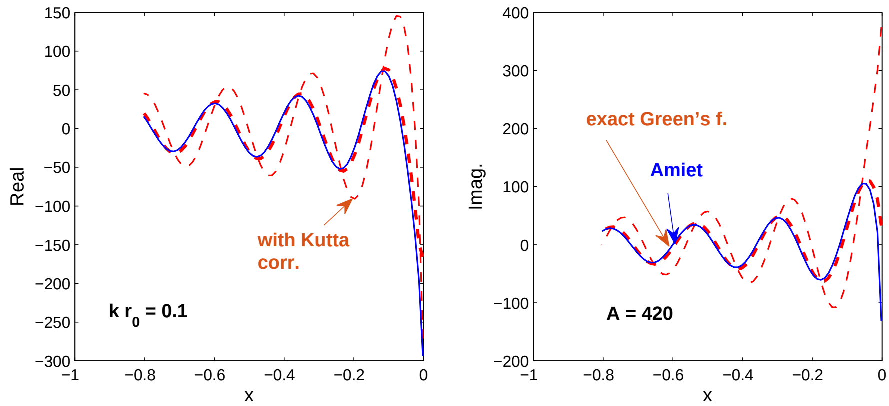

Figure 2: Real and Imaginary parts of the radiating wall pressure. Amiet's solution (blue), edge scattering of a point dipole with and without Kutta condition (thick and thin dashed red lines, resp.).

B. Expression of the Excitation

The direct sound field radiated from a point lift-dipole is also given by the scalar product of the dipole strength with the first gradient of the free-space Green's function with respect to the source coordinates. In the two-dimensional space of the study, the Green's function is expressed with the Hankel function. For a unit dipole strength the field reads

$$\frac{\partial G}{\partial y_0} = \frac{\mathrm{i}\, k\,(y_0 - y)}{4\,\beta\,\bar{R}}\, \mathrm{e}^{-\mathrm{i}\,K M_0\,X}\, \mathrm{H}_0^{(1)\prime}\left(K\,\bar{R}\right) = \frac{\mathrm{i}\,K\,(y - y_0)}{4\,\bar{R}}\, \mathrm{e}^{-\mathrm{i}\,K M_0\,X}\, \mathrm{H}_1^{(1)}\left(K\,\bar{R}\right)$$

where (x_0, y_0) and (x, y) stand for source and observer coordinates, respectively. $R = [(x-x_0)^2 + (y-y_0)^2]^{1/2}$ is the source to observer distance and $\bar{R}$ its expression with X instead of x. In the present case the trailing edge of a reference vane is located at the origin of coordinates. Because the unwrapped representation of the annular stator at radius r_c must be periodic of period $V\,h$ where V is the number of vanes and $h = 2\,\pi\,r_c/V$ is the channel width, the same point source must be repeated every V channels. This leads to the periodized field

$$p_0 = \frac{\mathrm{i}\,K}{4}\, \mathrm{e}^{-\mathrm{i}\,K M_0\,X} \sum_{n=-\infty}^{\infty} \frac{y + n\,V h}{[X^2 + (y + n\,V h)^2]^{1/2}}\, \mathrm{H}_1^{(1)}\left(K\, \left[X^2 + (y + n\,V h)^2\right]^{1/2}\right) \tag{4}$$

This two-dimensional field can be expanded as an infinite discrete set of oblique plane-wave modes in the form

$$p_0 = \mathrm{e}^{-\mathrm{i}\,K M_0\,X} \sum_{j=-\infty}^{\infty} \bar{a}_j^{\pm}\, \mathrm{e}^{\mathrm{i}\,(K_{x,j} X + K_{y,j} y)} \tag{5}$$

with

$$K_{y,j} = \frac{j\,2\,\pi}{V h}\,, \qquad K_{x,j} = \pm \left[K^2 - \left(\frac{j\,2\,\pi}{V h}\right)^2\right]^{1/2} .$$

Indeed each plane wave must also be periodic in the y direction with the period Vh. The $+$ sign holds for propagation in the downstream direction $(x > 0)$, the $-$ sign for the upstream direction $(x > 0)$. A true plane wave is obtained only if $K_{x,j}$ is real and positive, which corresponds to the cut-on condition $K > j\,2\,\pi/(V h)$. Otherwise the mode is said cut-off and the necessary condition of exponential decay is ensured by putting

$$K_{x,j} = \pm\,\mathrm{i} \left[\left(\frac{j\,2\,\pi}{V h}\right)^2 - K^2\right]^{1/2} .$$

Downstream propagation is considered first. Identifying both expressions of p_0 and making use of the orthogonality integrals of exponential modes leads to the expression of $\bar{a}_j^{+}$ as

$$a_j^{+} = \frac{\mathrm{i}\,K}{4\,V h}\, \mathrm{e}^{-\mathrm{i}\left[K^2 - (j\,2\,\pi/(V h))^2\right]^{1/2} X}$$

$$\times \sum_{n=-\infty}^{\infty} \int_0^{V h} \frac{y + n\,V h}{[X^2 + (y + n\,V h)^2]^{1/2}}\, \mathrm{H}_1^{(1)}\left(K\, \left[X^2 + (y + n\,V h)^2\right]^{1/2}\right) \mathrm{e}^{-\mathrm{i}\,j\,2\,\pi\,y/(V h)}\, \mathrm{d}y$$

$$= \frac{\mathrm{i}\,K}{4\,V h}\, \mathrm{e}^{-\mathrm{i}\left[K^2 - (j\,2\,\pi/(V h))^2\right]^{1/2} X} \int_{-\infty}^{\infty} \frac{t\, \mathrm{H}_1^{(1)}\left(K\,\sqrt{X^2 + t^2}\right)}{\sqrt{X^2 + t^2}}\, \mathrm{e}^{-\mathrm{i}\,j\,2\,\pi\,t/(V h)}\, \mathrm{d}t$$

The antisymmetric part of the integrand can be ignored since it integrates to zero. Integrating by parts then leads, after a further change of variable, to the simplified form

$$\bar{a}_j^{+} = \frac{j\,\pi\,X}{(V h)^2}\, \mathrm{e}^{-\mathrm{i}\left[K^2 - (j\,2\,\pi/(V h))^2\right]^{1/2} X} \int_0^{\infty} \mathrm{H}_0^{(1)}\left(K\,X\,\sqrt{1 + u^2}\right) \cos\left(j\,\frac{2\,\pi\,X}{V h}\,u\right) \mathrm{d}u$$

The integral is readily calculated by using the connection between $\mathrm{H}_0^{(1)}$ and the modified Bessel function K_0 such that[1]

$$\mathrm{K}_0(-\mathrm{i}\,\xi) = \frac{\mathrm{i}\,\pi}{2}\, \mathrm{H}_0^{(1)}(\xi)$$

and the result[10]

$$\int_0^{\infty} \mathrm{K}_0\left(\alpha\sqrt{\xi^2+\beta^2}\right)\,\cos\gamma\xi\,\mathrm{d}\xi \;=\; \frac{\pi}{2\,\sqrt{\alpha^2+\gamma^2}}\,e^{-\beta\sqrt{\alpha^2+\gamma^2}} \tag{6}$$

valid for complex numbers α and β of positive real parts and for any real number γ. Finally the coefficient is found as

$$\bar{a}_j^+ \;=\; \frac{j\,\pi}{(Vh)^2}\left[K^2-\left(\frac{j\,2\,\pi}{Vh}\right)^2\right]^{-1/2}\,. \tag{7}$$

As expected the expression does not depend on the coordinate x, which is ensured by a proper choice of the square root in Eq.(6). For the coefficient a_j^- the developments are the same except that x is negative and that now the $-$ sign is taken for K_{xj}. Since X can be replaced by $|X|$ in the integrals the same expression is found in the end, so that $\bar{a}_j^- = \bar{a}_j^+ = \bar{a}_j$. This is also expected from the upstream/downstream symmetry of the sources in the absence of flow. Equation (7) for the upstream-propagating waves allows defining a relevant excitation of the trailing-edge interface of a stator. Because they are plane waves, the classical matching procedure for two-dimensional bifurcated waveguides[13] applies, whatever the cut-on or cut-off conditions might be.

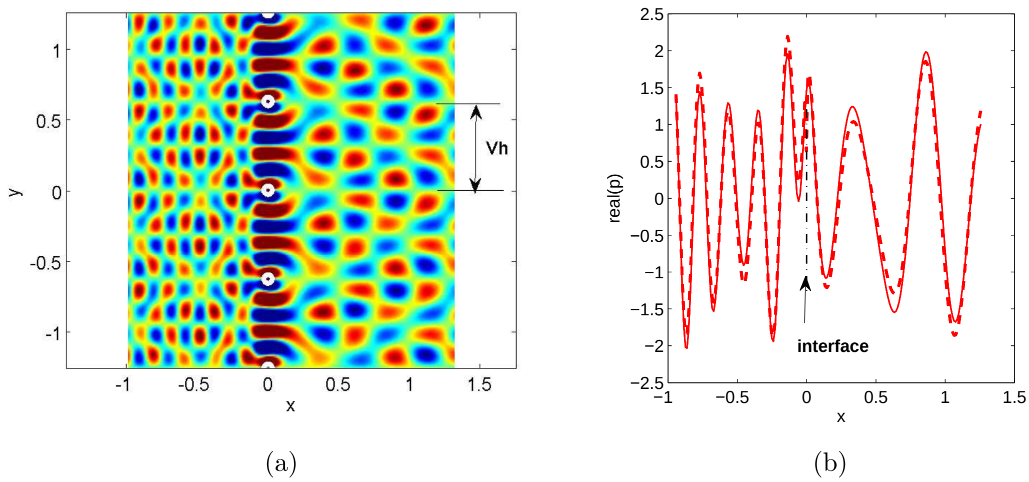

Figure 3: (a): simulated instantaneous sound pressure produced by a series of point dipoles; (b): pressure profiles predicted with the sum of Hankel functions (plain) and with the sum of plane waves (dashed). Helmholtz number $kVh = 17.4$, $U_0 = 100$ m/s.

Instantaneous pressure fields as calculated from Eq. (4) with the infinite sum of Hankel functions and from the sum of plane-wave modes with the coefficients of Eq. (7) are compared in Fig. 3. The pressure pattern, identical for both, is illustrated in Fig. 3-a, where the dipoles corresponding to a single trailing-edge source are indicated by the white circles. The flow is from left to right and the flat plates mimicking the vanes are not shown since the figure only deals with the direct field of the dipoles. The periodicity Vh is that of the unwrapped circular cut of the stator. Away from the near-field region surrounding the line of dipoles and not paying attention to the interference fringes, the sound field is of overall uniform amplitude in both directions. In contrast higher pressure fluctuations are seen in the vicinity of the sources. This is expected since the field is made of cut-off modes discernable close to the sources and cut-on modes which propagate without attenuation. A typical pressure profile along the line $y = 0.08$ is plotted in Fig. 3-b, where the continuous line stands for the sum of Hankel functions and the dashed line for the sum of plane-wave modes. The agreement confirms that the plane-wave expansion is relevant and can be used for the mode-matching technique. Moreover a large number of Hankel terms is needed to converge in Eq. (4) (300 in the present example) whereas a much smaller number of plane-wave modes is sufficient to reach the same convergence (with few differences between 10 and 30 terms). Yet residual discrepancies attributed to sum truncations, not prejudicial for the present application, are seen in the figure. The limited number of required plane waves is in favor of the present model.

III. Plane-Wave Scattering at Trailing Edge

A. Mode-Matching Procedure

Once the trailing-edge dipole is defined and the expansion in plane-wave modes performed, the scattering of each upstream-propagating plane wave by the trailing-edge interface of the stator is calculated using a mode-matching procedure. The theoretical background is inherited from fundamental techniques in bifurcated waveguide systems.[13] It has been simply extended to account for the presence of flow and applied by Ingenito & Roger[11] to address sound transmission problems at the axial inlet of a simplified centrifugal compressor. A generalization including hydrodynamic disturbances as incident waves and a Kutta condition at the trailing edges of a cascade of flat plates is also fully presented in a companion paper by Bouley *et al*[3] dealing with wake-interaction noise in axial-flow rotor-stator stages. The principle is described as follows for the primary scattering by the trailing-edge interface, first ignoring the Kutta condition, later introduced in sectionC. The incident oblique wave of index j forces transmitted cosine modes in the channels, of amplitudes A_m^j and shape functions $\cos(m\,\pi y/h)$, that propagate upstream, with a phase shift between adjacent channels imposed by the angle of incidence. A series of reflected, downstream-propagating waves of coefficients B_s^j and transverse phases $e^{\mathrm{i}\,\alpha_s^j y}$ with $\alpha_s^j = (j+sV)\,2\pi/(Vh)$ are also generated because the transverse periodicity of the incident wave is modulated by the periodicity of the cascade. All waves are matched at the interface by imposing continuity conditions. An infinite linear system of equations is obtained, solved by matrix inversion after being reduced by modal projection, or by any alternative method.

Though more general conditions could be required in the case of a mean-flow mismatch between both sides of the interface,[18] the continuity of fluctuating pressure and axial velocity is relevant in the present case of uniform axial flow. The acoustic potential ϕ is used as the primary variable from which the pressure and velocity are deduced as (for the convention $\mathrm{e}^{-\mathrm{i}\omega\,t}$)

$$p \;=\; \mathrm{i}\,\rho_0\,\omega\,\phi - \rho_0\,U_0\,\frac{\partial\phi}{\partial x}\,, \qquad\qquad v_x \;=\; \frac{\partial\phi}{\partial x}\,.$$

Any incident plane wave from downstream as defined in sectionB has the potential

$$\phi_i \;=\; a_j\,\mathrm{e}^{\mathrm{i}\,j\,2\pi\,y/(Vh)}\,\mathrm{e}^{-\mathrm{i}\,(K^{(j)}+M_0 K)X}$$

with

$$\bar{a}_j \;=\; \mathrm{i}\,a_j\,\frac{\rho_0 c_0}{\beta}\,\left(K + M_0 K^{(j)}\right) \qquad\qquad K^{(j)} \;=\; \sqrt{K^2 - \left(\frac{j\,2\pi}{Vh}\right)^2}$$

The transmitted potentials in the inter-vane channels are expressed as sums of cosine modes. Now adjacent inter-vane channels have phase-shifted responses driven by the obliqueness of the incident wave, in such a way that the coefficients in the channel of index ν are those of the reference channel ($\nu = 0$) multiplied by $\mathrm{e}^{\mathrm{i}\nu\,u}$ with $u = j\,2\pi/V$. As a result the transmission problem only needs being solved for the reference channel. In the latter the transmitted potential reads

$$\phi_t \;=\; \sum_{m=0}^{\infty} A_m^j\,\cos\left(\frac{m\,\pi y}{h}\right)\,\mathrm{e}^{-\mathrm{i}\,(K_m+M_0 K)X} \quad \text{with} \quad K_m \;=\; \sqrt{K^2 - \left(\frac{m\pi}{h}\right)^2}$$

Finally the reflected field is a sum of oblique plane waves written as

$$\phi_r \;=\; \sum_{s=-\infty}^{\infty} B_s^j\,\mathrm{e}^{\mathrm{i}\,\alpha_s^j\,y}\,\mathrm{e}^{\mathrm{i}\,(\bar{K}_s^j - M_0 K)X} \quad \text{with} \quad \bar{K}_s^j \;=\; \sqrt{K^2 - \alpha_s^{j2}}\,;\; \alpha_s^j \;=\; (j+sV)\,\frac{2\pi}{Vh}$$

If the trailing-edge interface is placed at $x=0$ in a first step the matching equations read

$$\sum_{m=0}^{\infty} A_m^j\,\cos\left(\frac{m\,\pi y}{h}\right) \;=\; a_j\,\mathrm{e}^{\mathrm{i}\,j\,2\pi\,y/(Vh)} \;+\; \sum_{s=-\infty}^{\infty} B_s^j\,\mathrm{e}^{\mathrm{i}\,\alpha_s^j\,y} \tag{8}$$

$$\sum_{m=0}^{\infty} (K_m + M_0 K)\, A_m^j \cos\left(\frac{m\,\pi y}{h}\right) \;=\; a_j\,(K^{(j)} + M_0 K)\,\mathrm{e}^{\mathrm{i}\,j\,2\pi\,y/(Vh)} \;-\; \sum_{s=-\infty}^{\infty} B_s^j\,(\bar{K}_s^j - M_0 K)\,\mathrm{e}^{\mathrm{i}\,\alpha_s^j\,y} \tag{9}$$

These equations are first reduced by projection on the modes of the inter-vane channels, considering only the reference channel $0 \leq y \leq h$ and the integrals

$$I_m^j \;=\; \int_0^h \mathrm{e}^{\mathrm{i}\,j\,2\pi\,y/(Vh)} \cos\left(\frac{m\,\pi y}{h}\right) \mathrm{d}y \qquad J_m^{s,j} \;=\; \int_0^h \mathrm{e}^{\mathrm{i}\,\alpha_s^j\,y} \cos\left(\frac{m\,\pi y}{h}\right) \mathrm{d}y\,,$$

keeping in mind that j cannot be zero in the present case. The following expressions are found for I_m^j:

$$I_m^j \;=\; \mathrm{i}\,\frac{j\,2\pi}{Vh}\,\frac{\left[1 - (-1)^m\,\mathrm{e}^{\mathrm{i}\,2\pi\,j/V}\right]}{\left(\dfrac{2\pi\,j}{Vh}\right)^2 - \left(\dfrac{m\pi}{h}\right)^2} \quad \text{if} \quad m \neq \pm\frac{2j}{V}$$

$$I_m^j \;=\; \frac{h}{2} \quad \text{if} \quad m = \pm\frac{2j}{V}$$

and similar ones are obtained for $J_m^{s,j}$ when replacing $j\,2\pi/(Vh)$ by α_s^j, with the value $h\delta_{0,m}$ if $j + sV = 0$.

Equations (8) and (9) lead to

$$A_m^j\,\frac{h}{2}\,(1 + \delta_{0,m}) \;=\; a_j\,I_m^j \;+\; \sum_{s=-\infty}^{\infty} B_s^j\,J_m^{s,j} \tag{10}$$

$$(K_m + M_0 K)\,A_m^j\,\frac{h}{2}\,(1 + \delta_{0,m}) \;=\; a_j\,(K^{(j)} + M_0 K)\,I_m^j \;-\; \sum_{s=-\infty}^{\infty} B_s^j\,(\bar{K}_s^j - M_0 K)\,J_m^{s,j} \tag{11}$$

Now the trailing-edge interface is also the source of the excitation in the present problem. Therefore, after the matching equations (10) and (11) are solved, the total field downstream of the interface must be cleaned of the incident plane wave and added to the complementary downstream-travelling component of the expansion illustrated in Fig. 3. The complete cascade trailing-edge scattering is obtained by summing the contributions of all oblique waves defined in section B.

B. Response of a Finite-Chord Stator

Section A only addresses the initial response of the stator trailing edges. The primary upstream-travelling waves forced in the inter-vane channels by the trailing-edge dipoles are next scattered at the leading-edge interface of the stator. This is accounted for by formulating there another mode-matching problem with the same continuity conditions. Part of the sound is radiated upstream and part is reflected back in the channels. That part experiences another trailing-edge scattering, which produces transmitted waves downstream and reflected waves in the channels, and so on. Finally four sets of waves are produced, namely open-space waves upstream and downstream of the stator and internal waves in both directions in the channels. Of course the phase-shift between adjacent channels imposed by the excitation is preserved in the full sound field so that again only a single reference channel needs being considered. This multiple scattering must be properly reproduced to accurately predict the cascade response and the possibly associated resonances.

The matching procedure is summarized as follows (see details in Bouley *et al*[3]). The trailing-edge interface is now located at $x = c$ where c is the chord length of the vanes and the leading-edge interface is located at $x = 0$. The four sets of waves are described by their acoustic potentials : the exhaust/reflected and inlet/transmitted potentials in the unbounded domains, referred to as ϕ_r and ϕ_t, and those in the inter-vane channels referred to as ϕ_u and ϕ_d for upstream and downstream propagation directions, respectively. The potential ϕ_r is written as

$$\phi_r = \sum_{s=-\infty}^{+\infty} R_s\,\mathrm{e}^{\mathrm{i}\alpha_s y}\,\mathrm{e}^{\mathrm{i}\bar{K}_s^{+}(X - c/\beta)}\,, \quad X \geq c/\beta \tag{12}$$

and the potential ϕ_t as

$$\phi_t = \sum_{s=-\infty}^{+\infty} T_s \, \mathrm{e}^{\mathrm{i}\alpha_s y} \, \mathrm{e}^{\mathrm{i}\bar{K}_s^- X} \, , \quad X \leq 0, \tag{13}$$

with $\bar{K}_s^{\pm} = -MK \pm \bar{K}_s^j$.

The potentials ϕ_u and ϕ_d in the reference inter-vane channel are expressed as

$$\phi_u = \sum_{m=0}^{+\infty} U_m^0 \, \cos\left[\frac{m\pi}{h} y\right] \mathrm{e}^{\mathrm{i}K_m^-(X-c/\beta)} \, , \qquad \phi_d = \sum_{m=0}^{+\infty} D_m^0 \, \cos\left[\frac{m\pi}{h} y\right] \mathrm{e}^{\mathrm{i}K_m^+ X} \, , \tag{14}$$

$$0 \leq X \leq c/\beta, \quad K_m^{\pm} = -MK \pm K_m \, .$$

For convenience, a vector $\mathbf{\Gamma}_q$ is introduced, having the pressure and axial velocity as components, $q = i, r, t, d, u$ denoting the incident (i), reflected (r), transmitted (t), downstream channel (d) and upstream channel (u) acoustic waves, respectively:

$$\mathbf{\Gamma}_q(x, y) = \begin{pmatrix} p(x, y) \\ v_x(x, y) \end{pmatrix} . \tag{15}$$

The continuity of pressure and axial velocity is imposed at the leading-edge interface ($x = 0$) and the trailing-edge interface ($x = c$). The matching equations result as

$$\mathbf{\Gamma}_i(c, y) + \mathbf{\Gamma}_r(c, y) = \mathbf{\Gamma}_d(c, y) + \mathbf{\Gamma}_u(c, y), \quad \forall y \tag{16}$$

$$\mathbf{\Gamma}_d(0, y) + \mathbf{\Gamma}_u(0, y) = \mathbf{\Gamma}_t(0, y), \quad \forall y \tag{17}$$

The system involves four unknown generic variables ($\mathbf{R}$, $\mathbf{D}^0$, $\mathbf{U}^0$, $\mathbf{T}$) and four matching equations. It could be solved at once, leading to a large matrix equation, but a sequential method is preferred for the sake of physical understanding. Two distinct matching problems are thus considered for both interfaces and solved iteratively. In the first step of the iterative procedure the first equation is solved with $\mathbf{\Gamma}_d = 0$ and $\mathbf{\Gamma}_u$ and $\mathbf{\Gamma}_r$ are calculated. In a second step the second equation is solved using $\mathbf{\Gamma}_u$ as excitation and now $\mathbf{\Gamma}_t$ and $\mathbf{\Gamma}_d$ are calculated. The first equation is solved again with all terms and so on. At every step a single interface is considered and only two vectors of coefficients ($\mathbf{R}$, $\mathbf{U}^0$) or ($\mathbf{D}^0$, $\mathbf{T}$) have to be determined, which makes the solving easier by matrix inversion. Furthermore the relative contributions of successive scattering orders can be more easily identified if needed. The iterative process is continued until all coefficients are converged.

C. Implementation of the Kutta Condition

In the presence of a mean flow, the fluctuating motion has to comply with the Kutta condition that imposes zero pressure jump at the trailing edges of the vanes. This condition significantly redefines the strengths of the scattered waves produced by the mode-matching technique, especially as the mean-flow Mach number increases, as pointed out by Bouley *et al.*[3] The same implementation as in the latter is carried out in the present study, bearing in mind that only the matching equations at the trailing-edge interface must be modified. In the mode-matching procedure the zero presure jump between both sides of a vane in the very near wake and farther downstream is automatically ensured by the continuity of the modal expansion in the unbounded domain. But a new constraint arises when it has to be specified also inside the inter-vane channels just upstream of the trailing edges, leading to an additional equation involving the vectors of modal amplitudes in the reference channel, written as

$$\sum_{m=0}^{\infty} (K - K_m^- M) \, [1 - (-1)^m \mathrm{e}^{-\mathrm{i}u}] \, U_m^0 = - \sum_{m=0}^{\infty} \mathrm{e}^{\mathrm{i}K_m^+ c/\beta} \, [1 - (-1)^m \mathrm{e}^{-\mathrm{i}u})(K - K_m^+ M] \, D_m^0 \tag{18}$$

Without any further modification this would end up with an over-determined linear system. But the Kutta condition results in the continuous shedding of vorticity in the wake. This is accounted for by distributing lines of concentrated vorticity in the continuation of the vanes. The strength of the vorticity vector in the direction normal to the unwrapped plane is expressed in the sense of generalized functions and reads

$$\Omega_K(x, y) = \Omega_0 \mathrm{e}^{\mathrm{i}KX/M_0} \sum_{\nu=-\infty}^{+\infty} \mathrm{e}^{\mathrm{i}\,\nu\, u}\, \delta(y - \nu h)\,, \quad X \geq c/\beta \tag{19}$$

where Ω_0 is a magnitude factor introduced as a new unknown. This vortical field is also expanded as a series of oblique gusts, in the form

$$\Omega_K(x, y) = \frac{\Omega_0}{h} \sum_{q=-\infty}^{+\infty} b_q\, \mathrm{e}^{\mathrm{i}KX/M_0} \mathrm{e}^{\mathrm{i}\alpha_q y}\,, \quad X \geq c/\beta \tag{20}$$

The associated velocity field $\mathbf{v}_K^h$ is obtained from the definition of the vorticity $\boldsymbol{\Omega}_K = \nabla \times \mathbf{v}_K^h$ and from its incompressibility ($\nabla \cdot \mathbf{v}_K^h = 0$). The expression of the axial velocity is given as:

$$v_{x,K}^h(x, y) = \sum_{q=-\infty}^{+\infty} \frac{\mathrm{i}\Omega_0 \alpha_q}{h\left(\alpha_q^2 + (K/M_0)^2\right)}\, \mathrm{e}^{\mathrm{i}KX/M_0}\, \mathrm{e}^{\mathrm{i}\alpha_q y}\,. \tag{21}$$

This hydrodynamic contribution is included in the matching equation for the axial velocity at the trailing-edge interface as an additional term in the $\mathbf{\Gamma}$ vector of Eq. (15). Because the hydrodynamic field is pressure-free, the matching equation for the pressure remains unchanged when the Kutta condition is imposed.

D. Scattering of Elementary Waves

Prior to full computations of edge-dipole scattering, inspecting the response of the cascade to elementary incident plane-wave modes from downstream allows highlighting fundamental properties of the cascade. This is achieved in this section for the unwrapped model stator shown in Fig.1, with a number of flat-plate vanes V=23 and an axial-flow Mach number of 0.15. The reference radius is r_c=0.08m. The selected frequency is 9 kHz, corresponding to Helmholtz numbers based on the channel height and on the vane chord of 3.6 and 7.5, respectively. At this frequency the channel modes of orders $m = 0$ and $m = 1$ are cut-on but higher-order modes are cut-off. This set of parameters typically corresponds to the small-size fans used in air-conditioning systems for aircraft. The results for the incident plane-wave modes $j = 9$ and $j = 11$ are investigated first and reported in Figs. 4 and 5. The left-side part of each figure shows an instantaneous pressure pattern and the right-side part displays the amplitudes of all modal coefficients as bar-graphs. Conventionally the incident mode has an upward phase speed.

The mode $j = 9$ (Fig. 4) is scattered into the modes $n = 9 \pm 23s$ both in the reflection and in the transmission, so that the lowest generated order except $n = 9$ is $n = -14$, noting that this mode is the first cut-off one in the present conditions. Therefore the upstream-transmitted wave is made of the mode 9 (or $s = 0$) only. The field (Fig. 4-a) is typical of the vicinity of the transition between a low-frequency regime for which only one mode is cut-on and a high-frequency regime for which two modes at least are cut-on away from the cascade. The reflection is quite strong and the field in the upstream vicinity of the cascade clearly exhibits an evanescent part. A secondary pattern with 5 periods is also visible around the cascade. The example of the mode $j = 11$ (Fig. 5) is featuring a clear transfer from the incident mode into another dominant mode in the upstream transmission, with inversion of the phase-speed direction. Indeed the scattered modes $n = 11$ and $n = -12$ are both cut-on but the latter ($s = 1$) is of much larger amplitude than the former ($s = 0$) in the upstream domain, as indicated by the diagram in Fig. 5-b. Reminding that the cascade is an unwrapped representation of a stator, this means that the dominant component of the transmitted wave is spinning in the opposite direction with respect to the incident wave. Still different behaviors could be described for other modes, not detailed here.

Because the excitation of the trailing-edge interface is produced by dipoles at vanishing distance from the edges in the present model, even the evanescent components of the oblique-wave expansion of section B contribute to the radiated field, as a result of modal scattering. But the same analysis as above in terms of isolated incident plane-wave modes for evanescent waves would be misleading because they would increase exponentially away from the cascade downstream. Such excitation modes need being analyzed by combining the opposite of the $-j$ component with the j component. Furthermore the downstream part of the excitation must be removed and replaced by the complementary downstream-emitted decaying wave. Such a test is

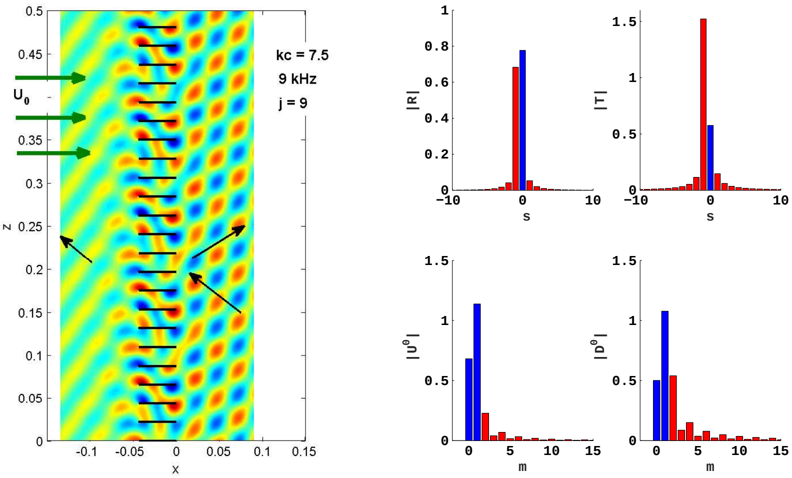

(a) (b)

Figure 4: Scattering of the incident plane-wave mode $j = 9$. (a): instantaneous sound pressure pattern. (b): modal coefficients, red for cut-off and blue for cut-on. $M_0 = 0.15$, $V = 23$, 9 kHz.

shown in Fig. 6 for the doublet of modes ($j = -17$, $j = +17$), again at the frequency of 9 kHz. Looking for the periodicity 17, the plot does not exhibit any radiating pattern but only a trace localized in the very vicinity of the vanes. Yet the scattering produces all modes of orders $n = \pm 17 - 23s$ and in particular the modes $n = +6$ and -6 ($s = -1$) that are cut-on at this frequency. This is why the latter contribute to the radiated field both upstream and downstream. For this reason a substantial number of cut-off modes must be included in the plane-wave expansion of the series of edge dipoles according to Eq.(5).

IV. Stator Broadband Noise Formulation

A. Scattered Field of an Edge Dipole

The complete response of the cascade for an edge-dipole at a single vane is determined by summing all plane-wave mode contributions according to Eq. (7). An *a priori* questionable point is that the coefficients $\bar{a}_j$ of the pressure waves do not tend to zero for arbitrarily increasing values of j. This is not prejudicial when synthesizing the direct pressure field in Fig. 3 since large values of j correspond to evanescent waves with increasing damping rates. But incident modes of large orders contribute when calculating the response of the stator because of the modal scattering. This is why a small but finite distance ε of the edge dipole to the trailing edge has been introduced and tested, the effect of which is to multiply the expression of $\bar{a}_j$ by the factor $\mathrm{e}^{\mathrm{i}\, K M_0\, \varepsilon}\, \mathrm{e}^{\mathrm{i}\, j\, \pi\, \varepsilon / [\bar{a}_j\, (V h)^2]}$. The small parameter ε must be such that $k\, \varepsilon \ll 1$ to ensure a proper tuning of the edge dipole by invoking the asymptotic behavior of the half-plane Green's function. Indeed the latter produces a strong amplification with the factor $(k\, \varepsilon)^{-1/2}$.[17] In contrast the coefficients a_j of the potential waves involved in the calculation of the acoustic powers do vanish for large values of j. It has been found that the results are not sensitive to the value of ε as long as it remains small (much less than one percent of chord in the present case), proving the robustness of the proposed approach.

A typical result combining all modes of orders j between -20 and 20 is plotted in Fig. 7-a in terms of instantaneous pressure, again for the same frequency of 9 kHz. The trailing-edge dipole is located on the center vane in order to emphasize the scattering by neighboring vanes. The two directly excited channels as well as the next two adjacent ones respond dominantly, whereas the pressure field is of much lower amplitude in more distant channels. As a result the upstream field exhibits two main oblique lobes that are fed by the four most excited channels, with secondary interference fringes. The obliqueness corresponds to spinning patterns in the annular space. The field downstream is substantially different because the dominant direction

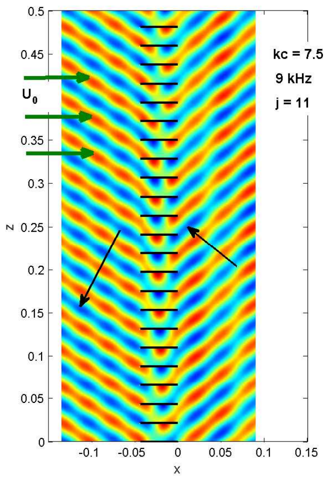

(a)

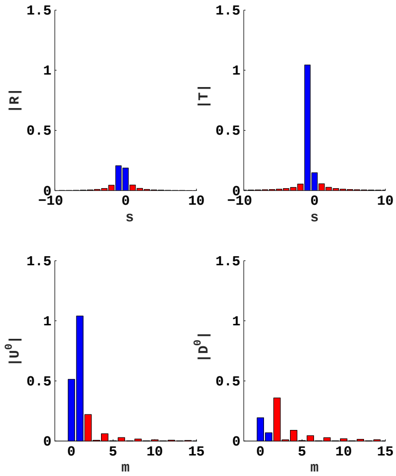

(b)

Figure 5: Scattering of the incident plane-wave mode $j = 11$. (a): instantaneous sound pressure pattern. (b): modal coefficients, red for cut-off and blue for cut-on. $M_0 = 0.15$, $V = 23$, 9 kHz.

of radiation of the edge-dipole is tangent to the trailing-edge interface.

B. Predicted Power Spectra

The same two-dimensional approach is now applied to demonstrate the feasibility of trailing-edge broadband noise predictions using the mode-matching technique, provided that the strength of the edge dipole is determined. For this some similarity is accepted with Amiet's model of isolated-airfoil trailing-edge noise, according to which the far-field sound is related to the statistical properties of the hydrodynamic wall-pressure field closely upstream of the trailing edge. More precisely the sound intensity is found proportional to the product $L\,\Phi_{pp}(\omega)\,\ell_y(\omega)$ where L is the spanwise extent, $\Phi_{pp}(\omega)$ is the hydrodynamic wall-pressure spectrum and $\ell_y(\omega)$ the associated spanwise correlation length.[16] The same is assumed here for the in-duct power at any frequency. Furthermore trailing-edge noise is not vane-to-vane correlated, so that the total acoustic power is the power from one vane multiplied by the number of vanes. Both Φ_{pp} and ℓ_y are required as input data. When they are unknown, empirical expressions proposed by many authors can be used, in terms of either outer or inner boundary-layer variables, accounting or not for the adverse pressure gradients characteristic of loaded airfoils (for a review see Rozenberg *et al*[19]). The present description cannot produce true quantitative results, precisely because the three-dimensionality is not addressed. Therefore only relative decibel levels are targeted, with emphasis on the intrinsic efficiency with which the cascade radiates upstream and downstream as a function of frequency. A corrected form of the expression proposed by Gliebe *et al*[7] for $\Phi_{pp}(\omega)$ and an empirical fit tuned on data reported by Guédel *et al*[9] for $\ell_y(\omega)$ are retained here for simplicity, essentially because they only require an estimate of the displacement thickness δ_1 as a minimum information. The corresponding formulae read

$$\Psi_{pp}(\omega) = \frac{\Phi_{pp}(\omega)}{\rho_0^2\,\delta_1\,U_0^3} = \frac{10^{-4}}{(1+0.3\,\bar{\omega}^2)^{5/2}}\,, \qquad \frac{\ell_y(\omega)}{\delta_1} = \mathrm{e}^{-2\,\bar{\omega}} + \frac{a}{\sqrt{\sqrt{2\,\pi}\,\sigma\,\bar{\omega}}}\,\mathrm{e}^{-(\ln\bar{\omega}-\ln 0.44)^2/(4\sigma^2)}$$

introducing the dimensionless frequency $\bar{\omega} = \omega\delta_1/U_0$, with $\sigma = 0.55$, $a = 1.5$.

It must be kept in mind that only the cut-on modes contribute to the power transmitted through the duct but that such modes can be generated by cut-off modes of the expansion in section B. The cut-off frequency of the first oblique wave in the unwrapped perimeter $2\pi\,r_c$ is 676 Hz for the mean radius of 80 mm in the present test case. Therefore no trailing-edge noise can be predicted below this frequency

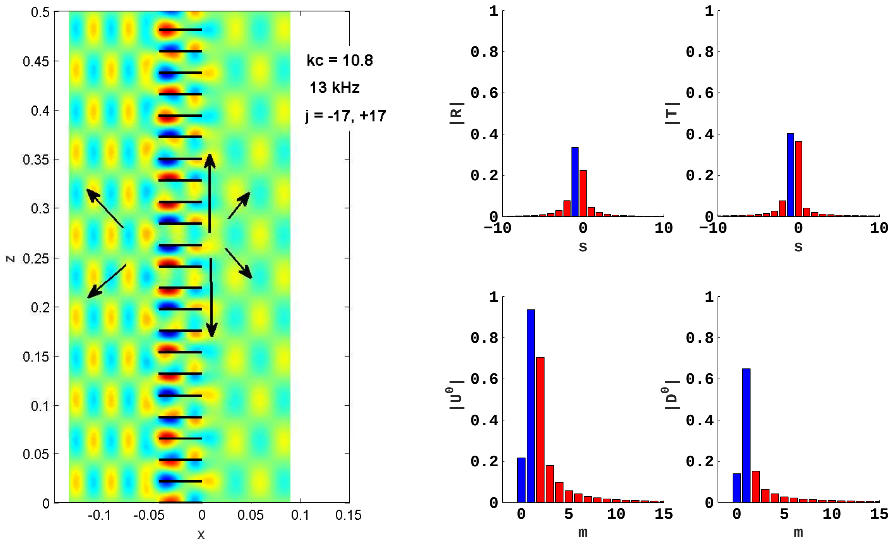

(a) (b)

Figure 6: Scattering of the combined incident modes $j = 17$ and $j = -17$ with source at the trailing-edge interface. (a): instantaneous sound pressure pattern. (b): modal coefficients for $j = 17$, red for cut-off and blue for cut-on. $M_0 = 0.15$, $V = 23$, 9 kHz.

because the edge dipole is oriented normal to the duct axis and cannot excite the axial plane-wave known to be always cut-on (the absence of any contribution from this wave can be recognized in Fig. 7-a). This limitation is inherent to the zero-stagger simplification. For staggered outlet guide vanes modeled by inclined flat plates the edge dipole would be inclined accordingly and would also excite the axial plane-wave mode. The limitation is not a serious issue because trailing-edge noise sources are weak at low frequencies, for which other sources would dominate in a real turbomachinery stage. Furthermore the excitation of the axial plane wave is more expected upstream than downstream where the vanes are actually aligned with the axis. Accounting for different stagger angles at the trailing edge and at the leading edge is a possible extension of the iterative mode-matching procedure. The extension would couple the model of sound propagation through bent ducts of slowly varying cross-section developed by Brambley & Peake[4] and Whitehead's theory of staggered waveguides.[20] In the present preliminary investigation the axial plane-wave mode is considered to negligibly contribute in the middle-and-high frequency range of major interest.

The classical definition of the acoustic intensity in a uniform base flow[8] is used to compute the acoustic power. For a potential of generic expression

$$\phi = \sum_{j=1}^{\infty} C_j \, \mathrm{e}^{\mathrm{i}\, j\, 2\pi\, y/(Vh)} \, \mathrm{e}^{-\mathrm{i}\,(\pm K^{(j)} + M_0 K) X}$$

away from the cascade the expression of the intensity reads

$$I = \mp k \, \beta^2 \, \rho_0 \, c_0 \sum_{j=1}^{\infty} |C_j|^2 \, K^{(j)}$$

where the $+$ and the $-$ signs correspond to downstream and upstream propagation, respectively. Predicted power spectra in a relative decibel scale, again for the same cascade configuration, are shown in Fig. 7-b. The plotted quantity is the power per unit span, radiated either downstream or upstream. The wall-pressure statistics is only used here to reproduce a realistic frequency distribution over the range 1 kHz-20 kHz, even though considering a spanwise correlation length within the scope of a two-dimensional theory is questionable.

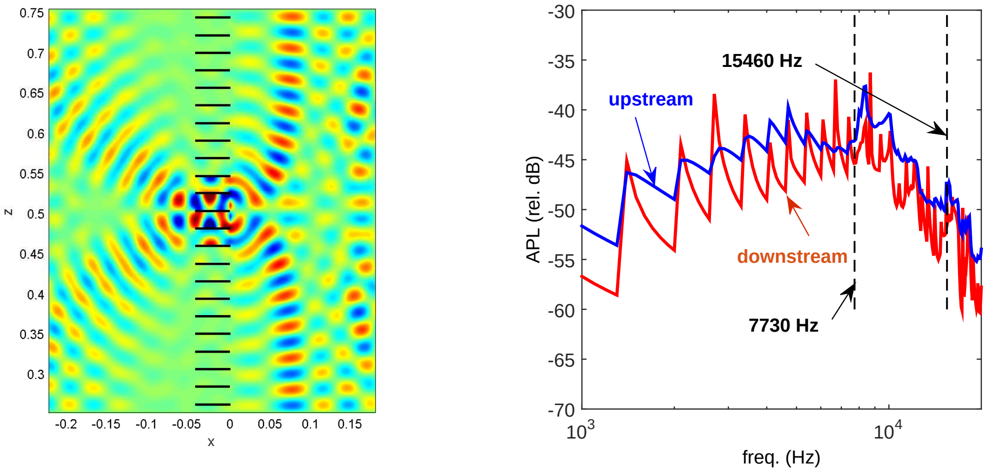

(a) (b)

Figure 7: (a): instantaneous sound pressure pattern for the diffraction of a single edge-dipole at the center vane ($\varepsilon = 0$). Flow from left to right, $M_0 = 0.15$, $V = 23$, 9 kHz. (b): downstream and upstream power spectra (per unit span and per vane). All plane-wave modes up to $|j| = 100$. Cut-off frequencies of the first two channel modes indicated as dashed lines.

The chord length is 45 mm and the displacement thickness at the trailling-edge is arbitrarily taken as 0.8 mm. The axial flow speed is of 50 m/s. The radiated power first increases with frequency and then decreases, as a result of the combined increasing acoustic efficiency and high-frequency energy drop in the involved hydrodynamic excitation. The cut-off frequencies of the first two transverse modes in the inter-vane channels of height 22 mm are 7730 Hz and 15460 Hz; they are indicated in the figure as vertical dashed lines. As expected from the analytical expression of the coefficients a_j peak responses are found at cut-off frequencies of the plane-wave modes away from the cascade. The peaks are especially marked downstream. Apart from these resonances the overall power level is predicted higher upstream than downstream by about 3 dB. This trend is compatible with the asymptotic cardioid radiation pattern of the trailing edge of isolated airfoils at high frequencies. Yet it could be questioned by cascade scattering. Furthermore considering staggered vanes would possibly redistribute the energy differently in the upstream and downstream directions because of the inclination of both the edge dipoles and the vanes. Indeed different trends are reported in the literature, based on experimental studies. As an example Woodward's work[21] in the case of a rotor with significantly staggered blades is cited here, bearing in mind that the experimental results were available for the rotor self-noise. If the latter is assumed to be essentially trailing-edge noise the same power was found to radiate upstream and downstream, at least in the low and moderate speed range of interest in view of the present investigation, whereas the opposite trend was observed at high speeds: much more sound was radiated downstream. Furthermore stator noise radiating upstream is partially reflected back downstream by the rotor blades, which is ignored in the present model but is inherent to all experimental results. Finally the present results are consistent.

Obviously the methodology is only relevant for large numbers of outlet guide vanes and large hub-to-tip ratios. Otherwise an approach currently used consists in splitting the annular cascade into a series of strips and unwrapping each strip to describe it as a two-dimensional cascade. Even if the radial extent of each annulus is defined in such a way that adjacent annuli are not correlated such an approach neglects the scattering of sources located at a radius by the walls at other radii. This is why the present formulation is only considered as a preliminary step. The mode-matching procedure can be easily extended to a true annular cascade in cylindrical coordinates, precisely taking benefit from the fact that the spanwise correlation length of the sources is generally much smaller than the duct height. Edge dipoles can still be defined and distributed along the trailing edges with their direct field expanded as a series of duct modes. The scattering of each mode by the full annular cascade can be determined exactly as long as the inter-vane channels can be considered as three-dimensional bifurcated waveguides. Such an extension is presently in progress. It will have the advantages of running without any expansion in strips and of avoiding the artificial parallelism of adjacent vane walls in the azimuthal direction.

V. Concluding Remarks

The new formulation proposed in the paper provides a simple way of solving the trailing-edge noise problem for a row of outlet guide vanes in an axial-flow fan architecture. The vanes are assimilated to a rectilinear cascade of zero-stagger plates in an unwrapped two-dimensional representation ensuring the periodicity of the stator. The first key step is the definition of a so-called edge dipole that is shown to be equivalent to the trailing-edge noise sources of a single vane at a given frequency. This dipole is approached at a vanishing distance to the edge from downstream. Its direct field is expanded into a series of plane-wave modes. In a second step the diffraction of each mode by the cascade is calculated considering the cascade as a periodic array of bifurcated waveguides and using a mode-matching technique. For this the mean flow is assumed uniform and a full Kutta condition is applied at the trailing edges. The total field of the dipole is obtained by summing all diffracted fields of the aforementioned plane-wave modes. It is also expressed as a series of modes, amongst which only the cut-on modes carry energy away from the cascade. The total acoustic power emitted by the stator is simply the power from one vane multiplied by the number of vanes. The finite chord length of the stator is a parameter of the model and the formulation holds for arbitrary subsonic Mach number and frequency.

Preliminary tests taking empirical wall-pressure statistics as input data have been made in a configuration of small-scale and low-speed axial fan. The results show that upstream radiation is typically 3 dB higher than downstream radiation. The practical tuning of the edge dipole is made by comparing the wall-pressure distributions produced by Amiet's model and by the half-plane Green's function for a lift dipole close to the edge. This means that the actual distance of the dipole to the edge is an important parameter entering the model. Moreover this distance is not uniquely defined: the smaller it is the smaller is the amplitude of the edge dipole. It has been verified that the sound power predictions do not significantly change if the edge dipoles are located at some finite distance ε instead of exactly at the trailing-edge interface, as long as the Helmholtz number $k\varepsilon$ remains much smaller than 1. This ensures the robustness of the model. Moreover the present estimates neglect the stagger angle of the vanes at the leading edge. Including this parameter in the analysis is identified as a first necessary extension.

The main advantages of the mode-matching technique are its formal simplicity and exactness in the considered geometry. It has large possibilities of extension that motivated the present effort. The two-dimensional extension to the case of staggered flat-plates is straightforward as long as adjacent vanes significantly overlap. The method can also be generalized in a three-dimensional context to address annular cascades of vanes in cylindrical coordinates without any need to resort to a strip theory, at least for unswept and untwisted vanes, which is a reasonable simplification in many designs. The extensions are currently in progress.

It is worth noting that channel modes or duct modes can also be defined for absorbing walls by replacing the underlying rigid-wall boundary condition by an impedance condition; this makes the mode-matching technique even more attractive.

Acknowledgements

The present developments have been partially made in the EC-funded project ACP2-GA-2012-314066 IDEALVENT (Integrated Design of Optimal Ventilation Systems for Low Cabin and Ramp Noise) and partially in the industrial chair ADOPSYS supported by SNECMA and the French Agency ANR.

References

[1] M. Abramowitz & I.A. Stegun, Handbook of Mathematical Functions, *Dover*, 1970

[2] R.K. Amiet, Noise due to turbulent flow past a trailing edge, *J. Sound Vib.* vol. 47(3), pp. 387-393, 1976.

[3] S. Bouley, B. François, M. Roger, H. Posson & S. Moreau, On a Mode-Matching Technique for Sound Generation and Transmission in a Linear Cascade of Outlet Guide Vanes, *21st AIAA/CEAS Aeroacoustics Conference, Aviation-2015*, Dallas, 2015.

[4]E. Brambley & N. Peake, Sound Transmission in Strongly-Curved, Slowly-Varying Cylindrical and Annular Lined Ducts with Flow, *12th AIAA/CEAS Aeroacoustics Conference*, paper 2006-2582, Boston 2006.

[5]S.A.L. Glegg, The response of a swept blade row to a three-dimensional gust, *J. Sound Vib.*, vol. 227(1), pp.29-64, 1999.

[6]S.A.L. Glegg & C. Jochault, Broadband self-noise from a ducted fan, *3rd AIAA/CEAS Aeroacoustics Conference*, Atlanta, 1997.

[7]P. Gliebe, R. Mani, H. Shin, B. Mitchell, G. Ashford, S. Salamah & S. Connell, Aeroacoustic prediction codes, *NASA-CR 2000-210244*, 2000.

[8]M.E. Goldstein, Aeroacoustics, *MacGraw-Hill* NY, 1976.

[9]A. Guédel, M. Robitu, N. Descharmes, D. Amor & J. Guillard, Prediction of the blade trailing-edge noise of an axial flow fan, *ASME Turbo Expo 2011*, paper GT2011-45256, Vancouver, 2011.

[10]I.S. Gradshteyn & I.M. Ryzhik, Tables of Integrals, Series and Products, *Academic Press N.Y.*, 1980.

[11]J. Ingenito & M. Roger, Analytical Modelling of Sound Transmission through the Passage of Centrifugal Compressors, *13th AIAA/CEAS Aeroacoustics Conference*, Rome, Italy, AIAA Paper 2007-3704, 2007.

[12]D.S. Jones, Aerodynamic Sound due to a Source Near a Half-Plane, *J. Inst. Maths Applics*, vol. 9, pp. 114–122, 1972.

[13]R. Mittra & S.W. Lee, Analytical Techniques in the Theory of Guided Waves, *McMillan, NY*, 1971.

[14]H. Posson, M. Roger & S. Moreau, On a uniformly valid analytical rectilinear cascade response function, *J. Fluid Mech.*, vol. 663, pp. 22-52, 2010.

[15]S. W. Rienstra, Sound diffraction at a trailing edge, *J. Fluid Mech.*, vol. 108, pp. 443–460, 1981.

[16]M. Roger & S. Moreau, Back-scattering and further extensions of Amiet's trailing-edge noise model; part I: theory, *J. Sound Vib.* vol. 286, pp. 477-506, 2005.

[17]M. Roger & S. Moreau, Edge scattering of distributed sources - application to high-lift device noise, *14th AIAA/CEAS Aeroacoustics Conference*, AIAA Paper 2008-2866, Vancouver, Canada, 2008.

[18]M. Roger, S. Moreau & A. Marsan, Generation and transmission of spiral acoustic waves in multi-stage subsonic radial compressors, *20th AIAA/CEAS Aeroacoustics Conference, Aviation 2014*, AIAA Paper 2014-3232, Atlanta GA, 2014.

[19]Y. Rozenberg, G. Robert & S. Moreau, Wall-Pressure Spectral Model Including the Adverse-Pressure Gradient Effects: Application to the Prediction of Trailing-Edge Noise, *AIAA J.*, **50 (10)**, pp. 2168-2179, 2012.

[20]E.A.N. Whitehead, The theory of parallel-plate media for microwave lenses, *Proc. IEE (London)*, **98**-III, pp. 133-140, 1951.

[21]R.P. Woodward et al., Fan Noise Source Diagnostic Test - Far Field Acoustic Results, NASA/TM-2002- 211591, 2002